A Fluidic Fuel Control System

BEN A. OTSAP* AND GEORGE A. YANKURA†
The Marquardt Corporation, Van Nuys, California

Requirements for the control system of a ramjet were established and used to design a fluidic fuel control system. The system consisted of a fuel mass flow rate sensor (fixed impedance type), an air mass flow rate sensor (variable impedance), an equivalence ratio computer, and a fuel throttling valve. Each component was tested before integration into a breadboard model. The integrated system was tested with air and with prospective ramjet propellants (air and hydrogen). With the exception of the mechanical fuel valve, all components performed within the established specifications. The fuel control system successfully metered the fuel over the entire ranges of air flow, engine inlet total pressure, and engine exit impedance in accordance with the equivalence ratio command that was inserted mechanically.

Nomenclature

a = sonic velocity
A = cross-sectional area
C_d = discharge coefficient
k = constant
K = constant
M = Mach number
P = pressure
R = gas constant
T = temperature
v = velocity
$\dot{W}$ = mass flow rate
Z = impedance to fluid flow, defined as $Z = P_T/\dot{W}$
α = constant denoting "fraction of"
ϵ = small increment
ϕ = equivalence ratio; ratio of fuel mass flow rate to air mass flow rate divided by the stoichiometric fuel-to-air ratio
γ = ratio of specific heats
$\|$ = variable denoting "fraction of"
ρ = density

Subscripts

a = air
c = control port
D = duct
= fuel; also used to label the output signal of the fuel/air ratio computer
N = labels the net output signal of the variable impedance mass flow rate sensor
p = probe
s = power supply of the variable impedance mass flow rate sensor
T = conditions at total, or stagnation, state; absence of subscript implies static conditions
Z = impedance
ϕ = Fuel/air ratio computer

Superscript

$*$ = conditions at sonic state

Presented at the AIAA 3rd Propulsion Joint Specialist Conference, Washington, D.C., July 17–19, 1967 (no paper number; published in bound volume of conference papers); submitted August 18, 1967; revision received February 16, 1968. This study was sponsored by the U.S. Air Force under Contract AF33-(615)-2399. The work was administered under the direction of Air Force Aeropropulsion Laboratory with H. C. Long as the Air Force Project Engineer.

* Manager, Fluid Control Research Group, Aerospace Products Division.

† Member of the Advanced Technical Staff, Aerospace Products Division.

Introduction

THE fuel control system in an air-breathing engine, and, in particular, a ramjet engine, requires a mass flow rate sensor to provide a signal proportional to the mass flow rate of the air without inducing a pressure drop in the air duct in obtaining the measurement. In addition, the sensor must be compatible with the rest of the control system. In turbojet engines, this is being accomplished by sensing the rpm of the compressor and relating it to the air flow rate. In ramjet engines, other techniques must be employed such as a mass flow measuring device[1] which samples a proportional amount of the duct flow and provides a pneumatic pressure signal proportional to it. The operation of such a device can be accomplished by using fluidic technology.

Ramjet engines have no moving parts and it would be very desirable to integrate a no-moving-part fluidic fuel control system in the operation of a ramjet engine. It will increase the reliability of the entire engine, reduce its weight, and extend its operating capabilities.[2]

A comparison of a moving-part (conventional) control system with extrapolated data for a comparable fluidic control system indicated that the fluidic system can be as much as an order of magnitude lower in size, weight, and cost and over an order of magnitude higher in reliability. Thus this investigation was conducted to determine the feasibility and practicality of fluidic technology to a fuel control system. A fuel control system is a basic control system for all air-breathing engines and the approach presented in this paper could therefore be adapted to ramjets as well as other air-breathing engines.

Description of Control System

The function of the fuel control system discussed in this paper is to maintain the fuel flow to the engine at a predetermined ratio to the air flow entering the engine combustor. A block diagram for this control system is shown in Fig. 1. The control system consists of the following components: a fluidic fuel mass flow rate sensor (fixed impedance type), a fluidic air mass flow rate sensor (variable impedance type), a fluidic fuel/air ratio computer, and a main fuel valve (conventional type).

The engine air mass flow rate is sampled by the variable impedance mass flow rate sensor which generates a net pneumatic pressure signal equivalent to the air mass flow rate, and applies it at the main fuel valve actuator, which serves as the summing junction. There, the net air flow signal is compared with the signal generated by the fuel mass flow rate

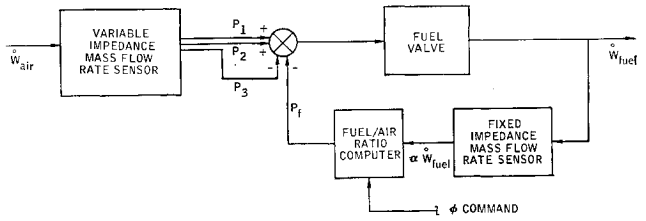

Fig. 1 Block diagram of feedback loop of fuel flow rate control system.

sensor (fixed impedance) and the fuel/air ratio computer. Any difference in the signals represents an error in the signals to the main fuel valve and causes the valve to modulate the fuel flow ratio until the error is nulled.

The mechanization of the control system is shown in Fig. 2. The output of the variable impedance mass flow rate sensor consists of three simultaneous pressure signals whose algebraic sum, the net pressure signal (P_M), is proportional to the engine intake air flow rate ($\dot{W}_a$). The fixed impedance mass flow rate sensor extracts a sample fuel flow ($\alpha\dot{W}_f$) which is proportional to the total fuel flow rate. This sample flow is fed through the fuel/air ratio computer whose output is a pressure signal (P_f) which is equivalent to the total fuel mass flow rate divided by the fuel/air equivalence ratio (ϕ). In practice, the setting of the fuel/air ratio computer could be fixed, made to follow a predetermined schedule, or be variable through feedback or external command. When the signal from the fuel/air ratio computer is equal to the net signal from the variable impedance mass flow rate sensor, i.e., when P_f equals P_N, then $\dot{W}_f$ will equal $\phi\dot{W}_a$. Consequently, the null condition results in the desired ratio of total fuel flow to intake air flow.

The signals from both mass flow rate sensors are affected by the fluid temperatures. Errors due to the temperature effect may be eliminated by the use of heat exchangers placed as shown in Fig. 2. In this application, it is not necessary that the heat exchangers achieve some reference temperature, only that they all achieve a common temperature. Therefore, a single four-channel heat exchanger could be used. This investigation was conducted at ambient temperature without the use of heat exchangers.

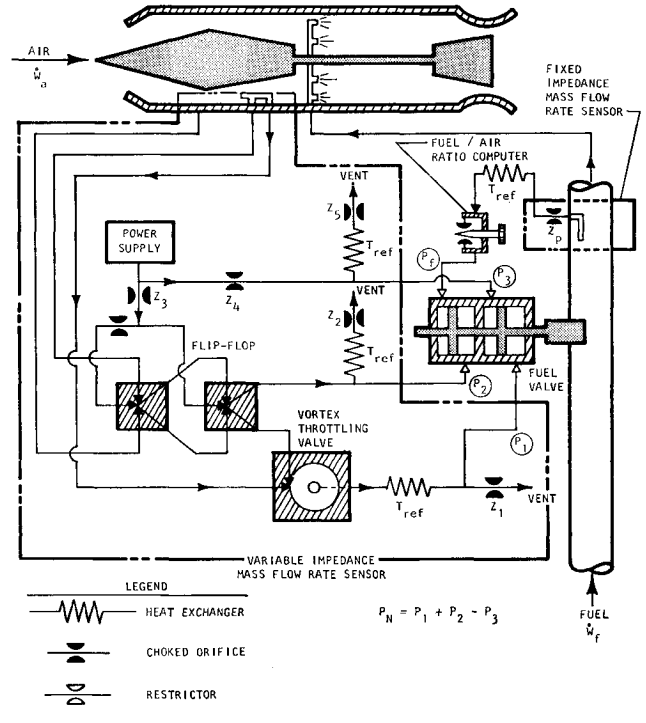

Fig. 2 Schematic of fuel control system.

System Components

Fixed Impedance Mass Flow Rate Sensor

The gaseous fuel flow rate is modulated by the main fuel valve which governs the fuel pressure upstream from the fixed and choked fuel injector orifice. Therefore, a probe placed in the fuel line and connected to a choked, fixed-area orifice will sample a probe flow rate that is a constant fraction of the fuel flow rate at all levels by virtue of the expression

$$\dot{W} = C_d A P_T f(\gamma,R,M)/(T_T)^{1/2} \quad (1)$$

Inasmuch as the Mach numbers in both the fuel line and the probe are constant due to the choked downstream impedances and since the fuel line and the probe are fed by the same total pressure and total temperature, the ratio of the probe flow rate to the fuel flow rate is always a constant.

Fuel/Air Ratio Computer

The fuel/air ratio computer is shown in Fig. 2 as a plenum with an adjustable orifice. The orifice operates in the choked condition, and thus the upstream pressure is proportional to the flow passing through it which comes from the fixed impedance mass flow rate sensor. Hence, this pressure is also proportional to the total fuel mass flow rate. Accordingly, it is utilized as the output signal (P_f) of the fuel/air ratio computer. The value of the constant of proportionality relating the signal and the total fuel flow rate determines the fuel/air ratio that the control system will maintain, and the constant is controlled by varying the effective area of the orifice. A needle valve was used in the fuel/air ratio computer in the breadboard control system.

Variable Impedance Mass Flow Rate Sensor

The variable impedance mass flow rate sensor samples a proportional amount of the air flow and generates a net pressure signal which is proportional to the total air mass flow rate. It accomplishes this under conditions of variable duct exit impedance, total pressure, and Mach number. The variable impedance mass flow rate sensor performs its

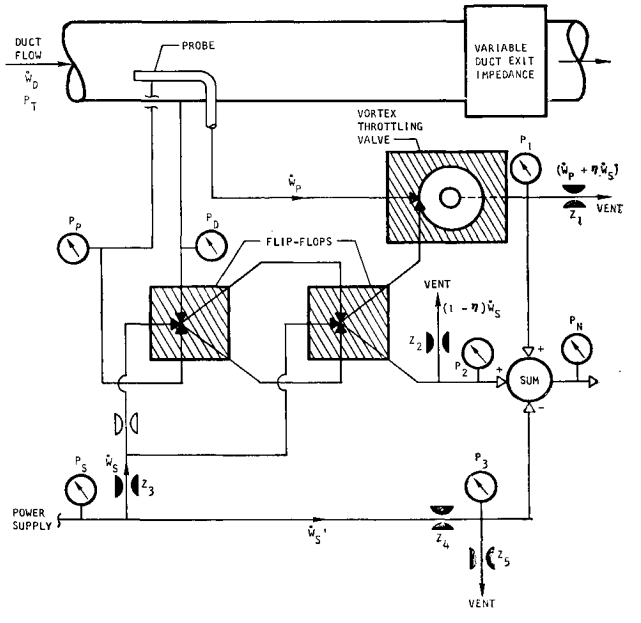

Fig. 3 Schematic of variable impedance mass flow rate sensor.

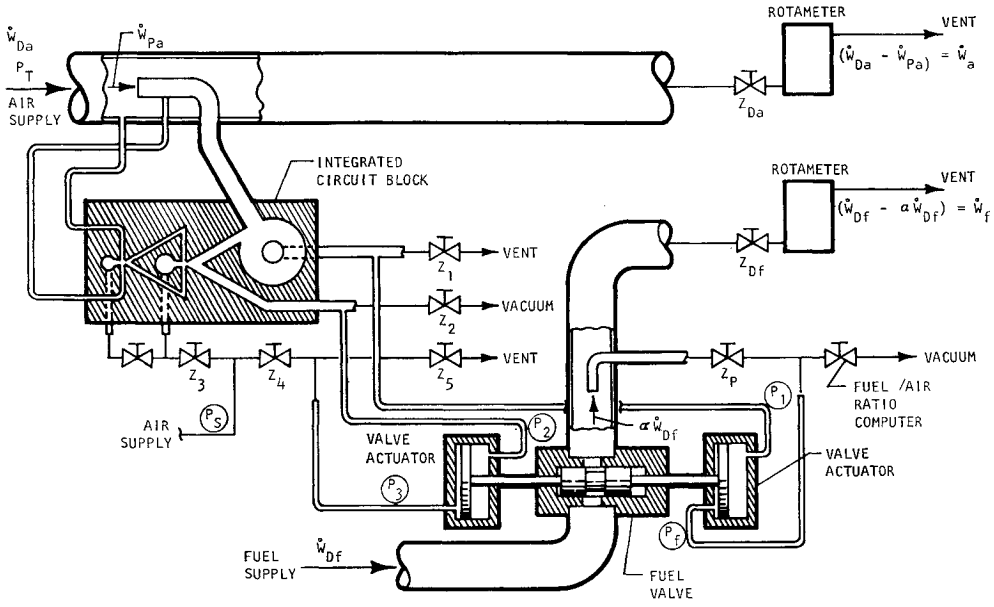

Fig. 4 Schematic of breadboard model of fluidic fuel/air ratio control system.

function by regulating the probe flow in a manner which maintains the probe static pressure equal to the duct static pressure, thus keeping the probe Mach number equal to the duct Mach number at all times. Therefore, the ratio of the probe flow rate to the duct flow rate is constant independent of duct impedance, total pressure, and Mach number.

Whereas the fixed impedance mass flow rate sensor is passive, the variable impedance mass flow rate sensor is active and requires a power source to function. The operation of the variable impedance mass flow rate sensor may be followed in the schematic of the fluidic mechanism presented in Fig. 3. The element in the sensor which controls the probe flow is the vortex throttling valve. This valve is switched on and off by digital amplifiers (flip-flops) which respond to the differential between the duct static pressure and the probe static pressure. Two flip-flops were staged, as shown, to improve the sensitivity of the sensor, or in other words, to decrease the differential between the probe and duct static pressures that would have to be attained before the sensor would respond.‡ When the output of the second-stage flip-flop is switched into the control port of the vortex throttling valve (valve on, or active mode), the probe flow is restricted. When the output of this flip-flop is switched out of the vortex throttling valve (valve off, or inactive mode), the probe flow is unrestricted.

The sequence of operation of the variable impedance mass flow rate sensor is as follows. Beginning with the duct and probe static pressures equal, and the vortex throttling valve in the off mode, the probe flow will increase because of the absence of restriction in the valve, and the probe static pressure will decrease. When the probe static pressure decreases to $(P_D - \epsilon)$ the output of the flip-flop will be switched into the vortex throttling valve and the valve will present a restriction to the probe flow. The probe flow will then decrease until the probe static pressure rises to $(P_D + \epsilon)$ when the output of the flip-flop will be switched out of the vortex throttling valve removing the restriction to the probe flow. The probe flow will then increase again and the probe static pressure will decrease and the cycle starts again. Beginning with the duct and probe static pressure equal and the vortex throttling valve in the on mode would obviously result in the same "limit cycle" action. In effect, the probe flow is pulse width modulated by the vortex throttling valve and its time average equals the amount corresponding to equal duct and probe static pressures. It only remains to convert the average probe flow into an equivalent pressure signal.

The flow out of the vortex throttling valve includes part of the output flow of the flip-flops in addition to the probe flow. Therefore, converting the output flow of the vortex throttling valve to a pressure signal would not accurately represent the total air flow in the duct. The problem was solved with a combination of three pressure signals as follows. The output flow of the vortex throttling valve is converted to the pressure signal (P_1) by means of the choked orifice Z_1. The part of the output flow of the flip-flop which bypasses the vortex throttling valve is converted to the pressure signal (P_2) by means of the choked orifice Z_2. The sum of P_1 and P_2 would represent the sum of the probe flow and the total power supply flow to the flip-flops. It is then only necessary to generate a third pressure signal (P_3) which is equivalent to the total supply flow and to subtract it from the sum of P_1 and P_2. The result would be a net pressure signal equivalent only to the probe flow and thus representative of the air duct flow. When the choked impedances Z_1 and Z_2 are made equal and when the power supply output is generated through a choked orifice, the pressure signal (P_3) may be generated using a pressure divider which also is composed of choked orifices. This is shown below. The orifices Z_4 and Z_5 make up the pressure divider. Therefore

$$P_1 = Z_1(\dot{W}_p + \eta \dot{W}_s) \tag{2}$$

and

$$P_2 = Z_2 (1 - \eta) \dot{W}_s \tag{3}$$

and also

$$P_s = Z_3 \dot{W}_s \tag{4}$$

The net pressure signal (P_N) is equal to

$$P_N = P_1 + P_2 - P_3 \tag{5}$$

since

$$\dot{W}_s' = P_s/Z_4 = P_3/Z_5 \tag{6}$$

$$P_N = Z_1 \dot{W}_p + \eta(Z_1 - Z_2)\dot{W}_s + [Z_2 - (Z_3 Z_5/Z_4)]\dot{W}_s \tag{7}$$

By making Z_1 equal to Z_2 and Z_2 equal to $(Z_3 Z_5/Z_4)$, the mass flow rate sensor generates a net pressure signal which is proportional to the probe flow, since Eq. (7) becomes

$$P_N = Z_1 \dot{W}_p \tag{8}$$

An aspect of the vortex throttling valve which must be considered in any application of the variable impedance mass

‡ With a single stage, the threshold differential was 3 psi; two stages reduced this to 0.3 psi.

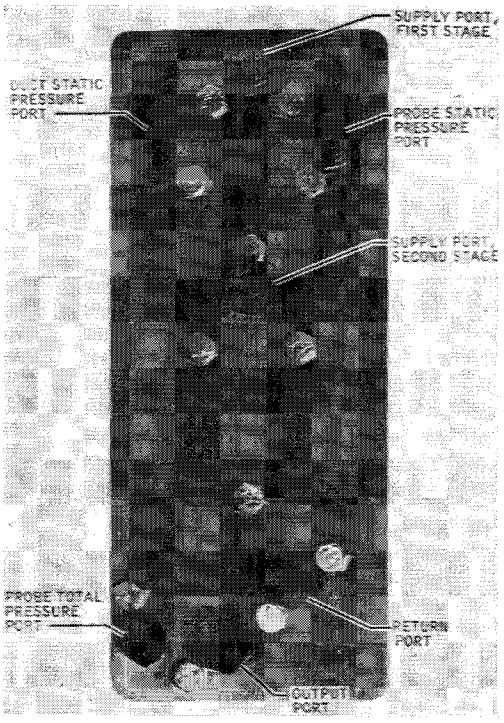

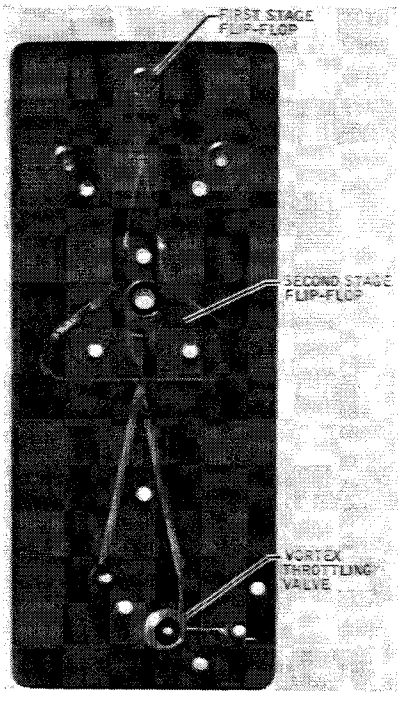

Fig. 5 Integrated circuit block for variable impedance mass flow rate sensor.

flow rate sensor is that in order to obtain the throttling action in the valve it is necessary to make the pressure in its control port greater than the pressure in its vortex chamber.[3,4] The power supply source for the flip-flops must be at a higher pressure than could be gotten by tapping it off the air stream. The power supply must then be provided through other means, such as an air-driven turbine compressor or simply an auxiliary onboard air supply.

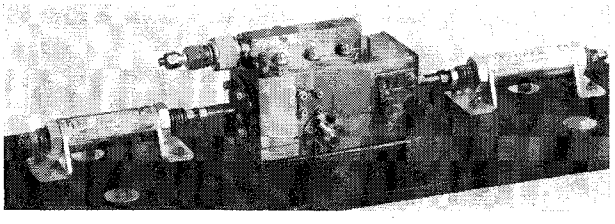

Fig. 6 Balanced piston design for fuel valve.

Experimental Investigation

Description of Test System

A breadboard test model was constructed and used to evaluate the performance potential of a fluidic fuel control system. Two ducts were used, to simulate the engine air intake duct and the fuel feed line, respectively. A schematic diagram of the breadboard model system is shown in Fig. 4. The breadboard model was tested at simulated operating conditions, first with air in both ducts (simulating fuel) and then with air and hydrogen. The test facility was capable of providing various entrance conditions at the fuel and air sides of the model. The fuel and air duct exit impedances were established by means of ordinary gate valves. The ranges of the conditions over which the breadboard fuel control system was tested were as follows: $0.08 < \dot{W}_a < 0.32$ pps (flow range of 4:1); $0.5 < \phi < 2.0$; $50 < P_{Ta} < 150$ psia; $500 < Z_{Da} < 650$ psi/pps.

The flip-flops and the vortex throttling valve of the breadboard model were fabricated as an integrated circuit as shown in Fig. 5. The close coupling achieved with the integrated circuit reduced interconnecting line "dead-space," thus increasing the limit cycle frequency of the variable impedance mass flow rate sensor. The integrated circuit block was connected to the sensor probe with lines made as short as possible. A balanced piston spool valve with two double-acting external actuators was used as the main fuel valve. The actuators were off-the-shelf air cylinders. The valve-actuator assembly is shown in Fig. 6.

Test Results

The variable impedance mass flow rate sensor was tested separately before being installed into the breadboard control system. The net pressure signal is P_N, where Eq. (5) was measured for various duct flow rates at several duct total pressures. The power supply pressure (P_s) was maintained at 2.85 times the duct total pressure. This multiple was found to provide the best performance over the range of test conditions. The relationship between the power supply pressure and the duct total pressure is discussed in Appendix A.

The results are plotted in Fig. 7. The initial plot of this data had more scatter than the plot shown here (see Ref. 2). The scatter was reduced after adjustment of the data for the variation of the coefficient of discharge with Reynolds number in the Z_1, Z_2, and Z_5 orifices. A representative correction

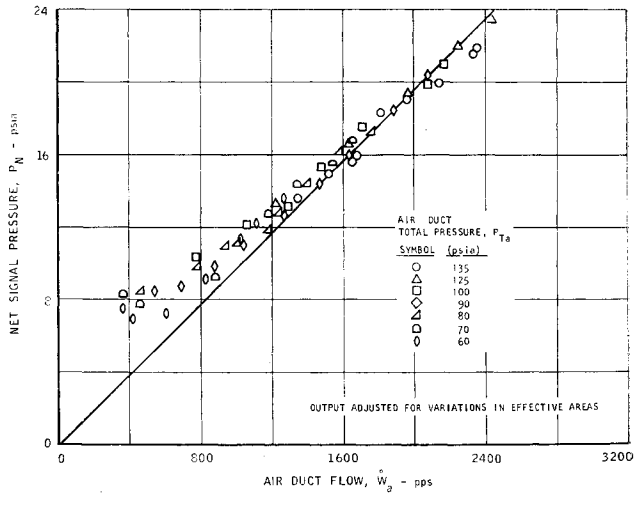

Fig. 7 Output of variable impedance mass flow rate sensor.

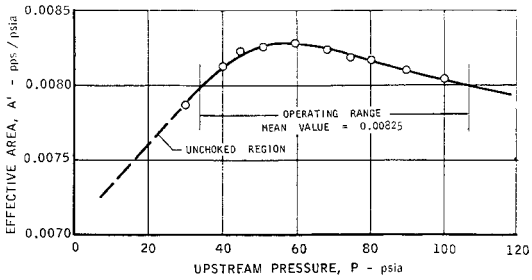

Fig. 8 Effective area characteristics for Z_1 and Z_2 orifices.

curve, used for the Z_1 and Z_2 orifices, which indicates the magnitude of the Reynolds number effect,[5] is shown in Fig. 8.

The data points in Fig. 7 fall progressively farther from a straight line through the origin as the duct flow is decreased below about 0.12 pps. This nonlinearity was due primarily to the nonlinear behavior of the needle valves used for orifices, especially near the limit at which they become unchoked.

The measured dynamic operating characteristics of the variable impedance mass flow rate sensor are shown in Fig. 9. The speed of response of the sensor to step changes in the input is given in this figure. The combination of the fixed impedance flow rate sensor, the fuel/air ratio computer, and the fuel valve was also tested separately, after which the breadboard control system was completed with the addition of the variable impedance mass flow rate sensor.

Results of tests of the complete breadboard control system, conducted with air in both ducts, are presented in Figs. 10 and 11. The results shown in Fig. 10 were obtained for three different settings of the equivalence ratio. The air duct exit impedance was constant whereas the air stream total pressure was varied. The test results confirmed that the control system does maintain the required fuel/air ratio for each setting of the fuel/air ratio computer.

The data presented in Fig. 11 are the results of tests in which the air duct exit impedance was varied. The air duct total pressure also was permitted to vary. In these tests, the variable impedance mass flow rate sensor power supply pressure (P_s) was controlled automatically, to follow the total pressure, by means of a Functionair in combination with a pneumatically controlled pressure regulator. The test schematic is shown in Fig. 12. The Functionair, an electropneumatic transducer, sensed the air stream total pressure

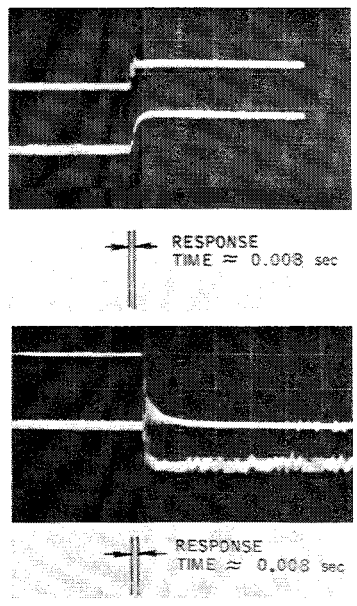

Fig. 9 Dynamic response time of variable impedance mass flow rate sensor.

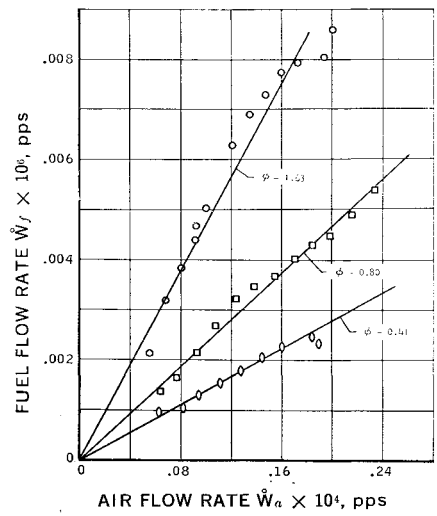

Fig. 10 Performance of breadboard fuel control system with varying air duct total pressure, using air as simulant fuel.

through a pressure transducer and applied a corresponding pneumatic signal to the pressure regulator supplying the variable impedance mass flow rate sensor power supply. The Functionair and the pressure regulator thus simulated the additional control loop mentioned earlier, which would be required in an actual application of the variable impedance mass flow rate sensor where the air stream total pressure varies. The tests were conducted at two fuel/air ratio settings. The leveling off of the fuel flow rate at the outer end of the plot, for ϕ equal to 1.45, was due to saturation of the fuel valve.

The flow rates plotted against air flow rate are shown in Figs. 13 and 14. These data are corrected for hysteresis due to stiction in the fuel valve. The deviations from the mean for the adjusted fuel vs air flow rate plot are $\pm 5\%$.

Analysis and Evaluation of Performance

The major cause of inaccuracy in the performance of the fuel control system was hysteresis. The major contributor of the hysteresis was the main fuel valve actuators which had excessive stiction and friction. The main fuel valve was constructed from off-the-shelf hardware and as a result, exhibited these undesirable characteristics.

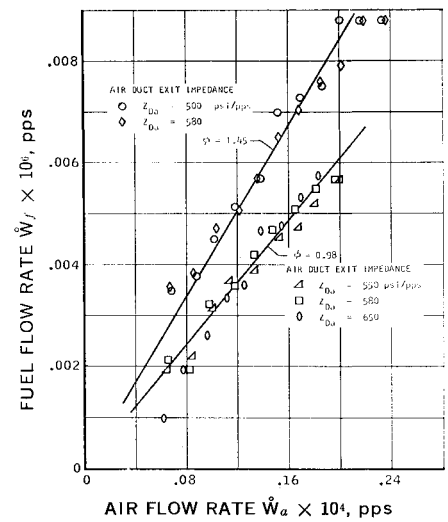

Fig. 11 Performance of breadboard fuel control system with varying air duct exit impedance and total pressure, using air as simulant fuel.

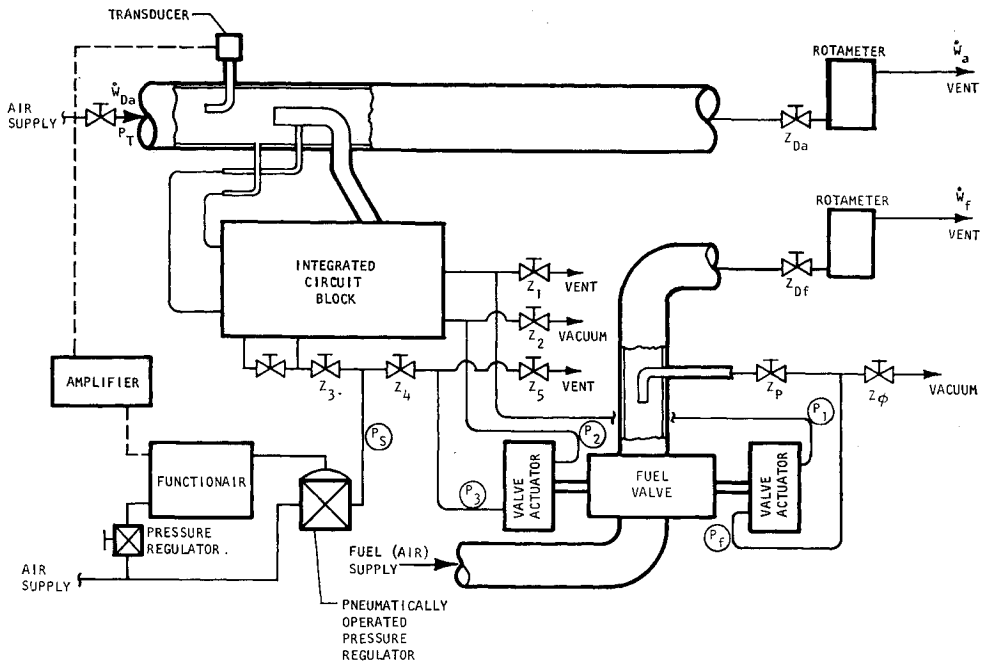

Fig. 12 Performance of breadboard fuel control system before adjustment, using air as simulant fuel.

A secondary source of inaccuracy was the variable impedance mass flow rate sensor. It is believed that the needle valves used in the sensor circuit in place of orifices were significant contributors. These would be replaced by nozzles in the final system.

In all of the data, the largest percentage deviations in the fuel/air equivalence ratio (ϕ) occur at the lower air flow rates. In the adjusted data, the performance deviations follow the deviations of P_N. Three factors which contributed to the errors in P_N were the use of needle valves for sonic orifices (discussed earlier), the operation of the breadboard system in the range of low sensitivity of the variable impedance mass flow rate sensor probe, and the data recording error. P_N is the algebraic sum of three recorded pressures, namely, P_1, P_2, and P_3. The pressures P_1 and P_2 were both oscillatory and although snuffers were installed in the lines to the pressure gages used to record them, some wavering remained. The pressure gage readings were recorded by still photography and, therefore, the readings which were obtained were not average readings. These errors, the last of which has no connection with the fuel control system, would be expected to influence the percentage deviations most at the lower air flow rates. Thus, the data points in the lower half of the air flow rate range should be excluded.

In conclusion, the evaluation of the results obtained from testing the breadboard fuel control system indicates an achieved accuracy of $\pm 5\%$ with air and hydrogen as the operating fluids when the effect of the interface valve hysteresis is adjusted out of the data and allowance is made for having used needle valves in place of proper sonic flow devices.

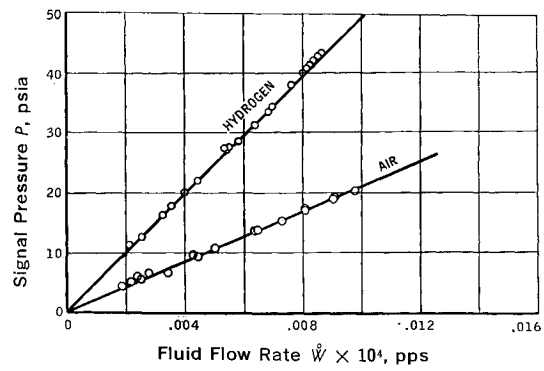

Fig. 13 Output of fixed impedance mass flow sensor.

Conclusions

The operation of a fluidic fuel control system for a ramjet engine has been demonstrated. The system maintained the required fuel/air ratio, based on an input command, over a range of air flow conditions as typically required by a ramjet engine.

It is estimated from the investigation that the power requirement in terms of fuel and air consumption, for this control system in a typical ramjet system application, would be about one-tenth of 1% of the total fuel and air flow. The characteristic behavior of the system was linear, although it possessed hysteresis. The amount of hysteresis can be reduced by replacing the sonic orifice devices used in the breadboard model with nozzles and by further investigation to optimize the system in terms of component dimensions and matching of impedances at the various nodes of the system. The state-of-the-art of fluidics is still at the stage where optimization must be accomplished by trial and error procedures. Further effort to develop a main fuel valve suitable for the requirements of the fuel control system would be necessary. Consideration should also be given to the possibility of the replacement of the fuel valve with fluidic components. The performance characteristics of the fluidic fuel

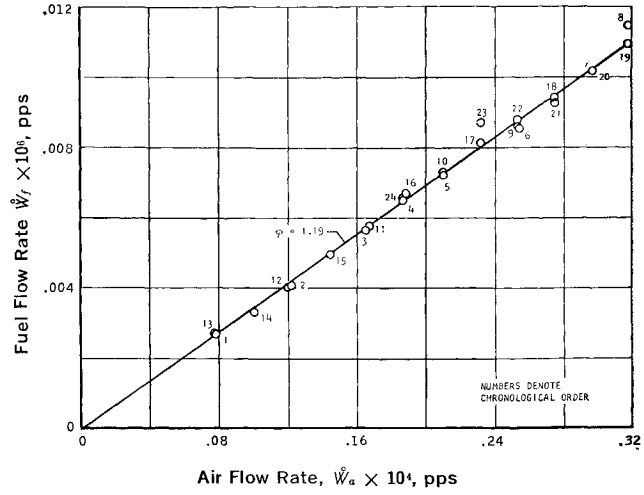

Fig. 14 Performance of breadboard fuel control system after adjustment, using hydrogen.

control system are independent of the type of fluid employed, provided the fluid is compressible and the operating conditions established in this investigation are met, such as adequate supply pressure level, choked fuel injectors, and equal fluid sample temperature.

Appendix A: Analysis of Operating Range

The operating range of the variable impedance mass flow rate sensor with respect to air stream total pressure (in the duct) air flow rate, and air duct exit impedance is governed mainly by the characteristics of the vortex throttling valve. Typical (somewhat idealized) characteristics are shown in Fig. 15. The solid characteristic lines represent the output flow of the vortex throttling valve. The dashed lines represent the supply flow, which in this case is the probe flow. Note that the vortex throttling valve is able to completely shut off the probe flow. Each characteristic gives the behavior of the vortex throttling valve as a function of the control port pressure (i.e., the output pressure of the flip-flop stage) at a fixed supply pressure. The supply pressure is related to the air duct total pressure. When the air duct Mach number is near zero, the supply pressure is equal to the total pressure for practical purposes. At greater Mach numbers, the supply pressure, which is approximately the probe static pressure, will be less than the total pressure.

Only the probe flow characteristics are shown in Fig. 16. In addition, two vertical lines are drawn to indicate the flip-flop output in the "off" position and the flip-flop output in the "on" position. The off output is assumed to be $3.5P$ and the on output is assumed to be $5.5P$. Assuming the supply pressure remains equal to the total pressure (true for low duct Mach numbers) and also that its value is $4P$, the probe flow will follow the portion of the $4P$ characteristic line between the vertical lines. Thus, the probe flow will vary between $5.2\dot{W}$ and $7.7\dot{W}$.

The bold horizontal line is drawn to indicate the average probe flow required to satisfy certain operating conditions. It is assumed to be $6.5\dot{W}$. Since the upper and lower flow rates (which the vortex throttling valve will accept from the probe) bracket the required average probe flow rate, the sensor can perform the limit cycle and regulate the probe flow.

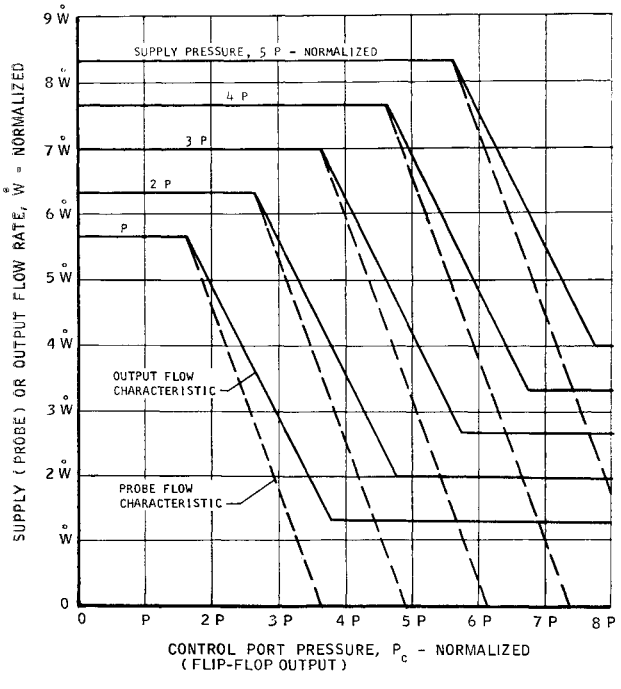

Fig. 15 Operating characteristics of the vortex throttling valve.

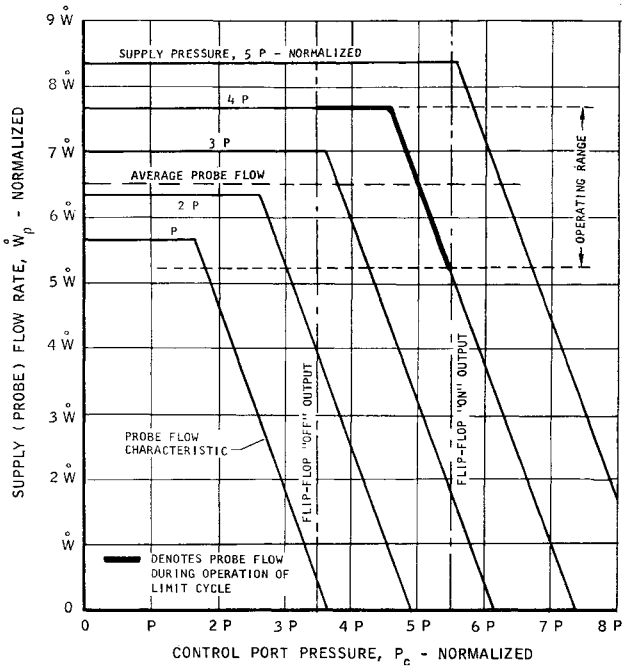

Fig. 16 Supply (probe) flow characteristics of the vortex throttling valve at constant supply pressure.

Should the duct impedance be decreased so that the required average probe flow rate exceeds $7.7\dot{W}$, the probe static pressure can never be made less than the duct static pressure, and the limit cycle action will cease. Likewise, should the duct impedance be increased so that the required average probe flow rate becomes less than $5.2\dot{W}$, the probe static pressure can never exceed the duct static pressure, and the limit cycle action will cease. However, in the latter case, should the on output of the flip-flop stage be simultaneously increased (by raising the pressure of the sensor power supply) the range of duct exit impedance would be extended. With respect to sustaining the operation of the limit cycle, the range of the variable impedance mass flow rate sensor in the direction of increasing air duct exit impedance can be extended indefinitely. However, with respect to the sensor output signal this is not so. As seen in Fig. 15, the output flow of the vortex throttling valve cannot be decreased beyond some minimum level (depending on the supply pressure) as can the probe flow. It should also be kept in mind that raising the on output of the flip-flop stage would raise the minimum (lower) cutoff of each output characteristic.

The total pressure range over which the variable impedance mass flow rate sensor will operate is affected in the following manner. Let the duct exit impedance be fixed. Then as the total pressure varies, so will the duct flow rate (it will be assumed here that they are linearly related). The operating limits for the sensor are then as shown in Fig. 17. For total pressures greater than $4.6P$, the required average probe flow rate will exceed $7.5\dot{W}$, the upper horizontal line in the figure, and the vortex throttling valve (which is constrained by the flip-flop output to operate between the vertical lines) cannot decrease the probe flow sufficiently. However, if the on output of the flip-flop is again increased as the total pressure increases, the operating range of the variable impedance mass flow rate sensor will be extended to higher total pressures. Eventually, a limit will again be reached when $\dot{W}_P$ equals $8.47\dot{W}$. Now the upper cutoff of the vortex throttling valve prevents the probe flow from being increased further to match the duct flow. For total pressures less than $1.6P$, the required average probe flow will be less than $2.6\dot{W}$, the lower horizontal line in Fig. 17. Now the vortex throttling valve cannot increase the probe flow sufficiently unless the off output of the flip-flop is decreased. Here also a second limit will eventually be reached when the output flow

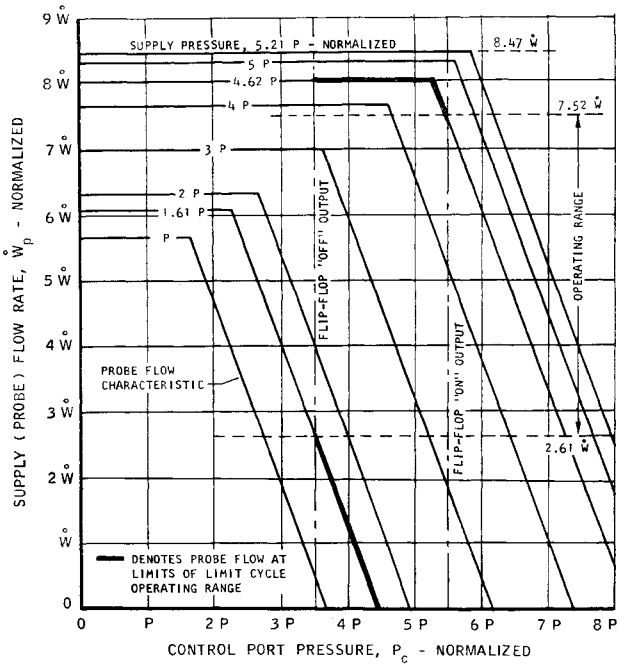

Fig. 17 Supply (probe) flow characteristics of the vortex throttling valve at constant duct exit impedance.

rate of the vortex throttling valve cannot be decreased further.

In situations where the duct Mach number is sufficiently greater than zero (but less than unity) and the supply pressure is significantly lower than the total pressure, the behavior of the probe flow rate with respect to the control pressure (flip-flop output) will not follow the constant supply pressure characteristics. Rather, as the probe flow is throttled, the supply pressure will increase (but can never exceed the total pressure), and as the probe flow is unthrottled, the supply pressure will decrease.

One further item that must be dealt with in the matching of the variable impedance mass flow rate sensor to a specific application is the size of the impedance placed downstream from the vortex throttling valve, i.e., Z_1 in Fig. 3. This impedance determines the upper cutoffs of the probe flow characteristics. It must therefore be selected so that these cutoffs would occur at higher probe flows than would be required in operation. At the same time, it must not be so small as to unchoke above the minimum vortex throttling valve output flow that will occur in operation. Here the ambient pressure is important.

References

[1] Chamberlain, "Mass Flow Measuring Device," U.S. Patent 2,780,938, Feb. 1957.

[2] Otsap, B. A. and Yankura, G. A., "Application of Fluidics to Ramjet Control System," presented at the SAE Aerospace System Conference, June 1967.

[3] Mayer, E. A. and P. Mulser, "Control Characteristics of Vortex Valve," presented at the Fluid Amplification Symposium, May 1964.

[4] Gerber, I. et al., "Fluid Vortex Amplifier Optimization," *Proceedings of the Fluid Amplification Symposium*, Case Institute of Technology, Oct. 1965.

[5] "Standard for Discharge Measurements with Standardized Nozzles and Orifices," TM 952, Sept. 1940, NASA.